Rate Constants for Quenching and Self-Annihilation of NCl($a^1\Delta$)†

Anatoly V. Komissarov,‡ Gerald C. Manke II,§ S. J. Davis,|| and Michael C. Heaven*,‡

Department of Chemistry, Emory University, Atlanta, Georgia 30322, Air Force Research Laboratory, Directed Energy Directorate, Kirtland AFB, New Mexico 87118, and Physical Sciences, Inc., 20 New England Business Center, Andover, Massachusetts 01810

Received: February 19, 2002; In Final Form: June 11, 2002

Quenching and self-annihilation rate constants for NCl(a) have been determined using pulsed 248 nm photolysis of ClN_3 to generate the metastable. Previous quenching measurements that employed different sources for NCl(a) yielded dramatically different rate constants. The present study provided quenching rate constants for Cl_2, HCl, and H_2 that are in good agreement with the discharge flow measurements of Hewett et al. (*J. Phys. Chem. A* **2000**, *104*, 539). Determination of the self-annihilation rate constant required knowledge of the branching fraction for NCl(a) formation for 248 nm photolysis of ClN_3. This information was obtained from time-resolved measurements of NCl(X) formation and decay. A lower bound for the branching fraction of 0.7 was determined. Self-annihilation of NCl(a) was studied by using intense photolysis pulses to generate high concentrations of NCl(a). Analysis of the second-order decay component yielded a rate constant of $(7.0 \pm 1.5) \times 10^{-13}$ cm^3 s^{-1}. This value is an order of magnitude smaller than the previous estimate (Henshaw et al. *J. Phys. Chem. A* **1997**, *101*, 4048).

Introduction

Interest in the possibility of using NCl(a) as an energy carrier in laser systems has motivated several studies of NCl(a) energy transfer and quenching kinetics.[1−11] These investigations indicated that an NCl(a) driven iodine laser was feasible,[6,12−14] and provided data that was essential for the design of a prototype device. This effort led to the recent demonstration of a chemically pumped iodine laser that relies on NCl($a^1\Delta$) as the primary energy carrier.[15] As many of the reactions occurring in this device have yet to be characterized, the laser demonstration has stimulated new efforts to understand the kinetics of NCl(a) generation and destruction.[16−18]

In previous kinetic studies two different experimental techniques were used to determine NCl(a) quenching rate constants, and the results appeared to be strongly dependent on the technique used. Hewett et al.[10] performed measurements in a discharge flow system. NCl(a) was generated from the reaction $Cl + N_3 \rightarrow NCl(a) + N_2$ and the intensity of the NCl $a-X$ system was monitored as a function of quenching gas density and time under steady-state conditions. Alternatively, Ray and Coombe,[5] and Henshaw et al.[9] used pulsed 193 nm photolysis of ClN_3 to generate NCl(a), and time-resolved fluorescence measurements to determine quenching rate constants. The photolysis experiments were performed in flow cells to avoid complications resulting from the build-up of photoproducts.

Ray and Coombe[5] reported that NCl(a) generated by 248 nm photolysis of ClN_3 has a complex time profile. Under certain conditions they found that the NCl(a) signal could show rise-fall characteristics. This behavior was attributed to secondary generation of NCl(a) from chain decomposition of ClN_3. Chain decomposition did not appear to be of importance when 193 nm photolysis was used. Instead, biexponential decays were observed. The long-lived component of the decay was attributed to NCl(a). Ray and Coombe,[5] and Henshaw et al.[9] determined NCl(a) removal rate constants by observing the dependence of the long-lived decay rate on the pressure of added quenchers or reactants. The level of agreement between the rate constants reported by the groups using photolysis generation was good, but several of the constants were dramatically different from the values measured in the discharge flow system. We recently reexamined the photolysis technique, with the intention of resolving the conflicts for the rate constant values.[17] In contrast to the work of Ray and Coombe,[5] we were unable to find evidence for secondary photochemical generation of NCl(a) when photolyzing ClN_3 at 248 nm. In fact, we found that 248 nm photolysis was the better source of NCl(a) for experiments that relied on detection via the $a-X$ emission band at 1.08 μm. Both 193 and 248 nm photolysis generate trace quantities of $N_2(B)$,[19] which is readily observed via a $B-A$ emission band at 1.04 μm.[9,17] Although the amount of $N_2(B)$ formed is small, it poses a problem because the N_2 $B-A$ transition moment is several orders of magnitude greater than the NCl $a-X$ transition moment. The ratio of NCl $a-X$ vs N_2 $B-A$ emission was much better for 248 nm photolysis, making it easier to reject interference from the latter. Our preliminary study of NCl(a) quenching kinetics[17] using 248 nm photolysis yielded rate constants that were in agreement with the flow tube results of Hewett et al.[10]

Self-annihilation of NCl(a), represented by the general reaction

$$NCl(a) + NCl(a) \rightarrow \text{products} \qquad (1)$$

constrains the density of NCl(a) that can be generated by chemical means, and the ability of the metastable to transport energy in a flow system. Hence, this parameter is of critical importance for NCl(a) driven laser systems. Henshaw et al.[9] measured the rate constant for reaction 1 using 193 nm

† Part of the special issue "Donald Setser Festschrift".
* To whom correspondence should be addressed.
‡ Department of Chemistry.
§ Air Force Research Laboratory.
|| Physical Sciences, Inc..

10.1021/jp0256645 CCC: $22.00
Published on Web 07/16/2002

photolysis of ClN_3 to generate high concentrations of NCl(a). As their results for quenching of NCl(a) were called into question by the studies of Hewett et al.[10] and Komissarov et al.,[17] we decided that a redetermination of the self-annihilation rate constant was required. The self-annihilation process cannot be observed under pseudo first-order conditions. To extract the rate constant from second-order decay data, the absolute concentration of NCl(a) immediately after the photolysis pulse (denoted as $[NCl(a)]_0$ in the following text) must be known. Henshaw et al.[9] used titration of NCl(a) by Br_2 to estimate $[NCl(a)]_0$. This is a valid procedure provided that NCl(a) is removed by reaction with Br_2, and that the reaction is rapid. Henshaw et al.'s[9] measurements indicated that the latter condition was met ($k_{Br_2} = 1.4 \times 10^{-11}$ cm^3 s^{-1}), but the rate constant reported by Hewett et al.[10] was an order of magnitude smaller, raising doubts about the validity of the titration.

In the present study we have used a different approach to determine the initial concentration of NCl(a). High photolysis laser irradiances were used to achieve conditions where 95% or more of the ClN_3 was photodissociated. The initial concentration of NCl(a) could then be obtained from the ClN_3 concentration, provided that the branching fraction for production of NCl(a) was known. The possible products for single photon dissociation at 248 nm are

$$ClN_3 + 248\ \text{nm} \rightarrow NCl(a^1\Delta) + N_2 \quad (2a)$$

$$NCl(X^3\Sigma^-) + N_2 \quad (2b)$$

$$NCl(b^1\Sigma^+) + N_2 \quad (2c)$$

$$Cl + N_3 \quad (2d)$$

Previous studies indicate that reaction 2a is the dominant channel.[4−6,9] The contribution from reaction 2c is relatively easy to evaluate, as formation of NCl(b) produces red emission from the $b-X$ band system. Comparison of the $a-X$ and $b-X$ emission intensities indicates that reaction 2c accounts for approximately 1% of the NCl formed. Quantitative studies of reaction 2d have not been reported. Photolysis of the isovalent species HN_3 via the equivalent absorption band yields H+N_3 with a branching fraction of 4%.[20] We have briefly examined photolysis of ClN_3 using time-of-flight mass spectrometry to detect the products.[21] For 193 nm photolysis we observed a small quantity of N_3, but there was no signal for this product when 248 nm photolysis was used. On the basis of this result, and the corresponding behavior of HN_3, we estimate that the branching fraction for reaction 2d is less than 10%. As NCl(a) and NCl(X) are the dominant photoproducts, we needed to know the branching fractions for these channels in order to determine $[NCl(a)]_0$. This information was obtained by observing transient absorption signals for NCl(X) when collisions of NCl(a) with $O_2(X)$ were used to transfer population from the initially formed NCl(a) to NCl(X).[1,5]

In the following sections we report quenching rate constant measurements for NCl(a), a determination of the NCl(a)/(NCl(a) + NCl(X)) branching fraction, and measurement of the rate constant for self-annihilation of NCl(a). As noted in our preliminary report, the quenching rate constants were in agreement with the results of Hewett et al.[10] Our self-annihilation rate constant is an order of magnitude smaller than the value reported by Henshaw et al.[9]

Experimental Section

Chlorine azide was formed by passing a mixture of 5% Cl_2 in He over the surface of moist NaN_3, in an apparatus similar to that described by Henshaw et al.[9] A standard drying agent was used to remove water from the ClN_3/Cl_2/He mixture at the exit of the generator. The concentration of ClN_3 was monitored via the absorption band at 250 nm. After the generator had been run for a few hours, the efficiency for converting Cl_2 to ClN_3 was in the range of 90−95%.

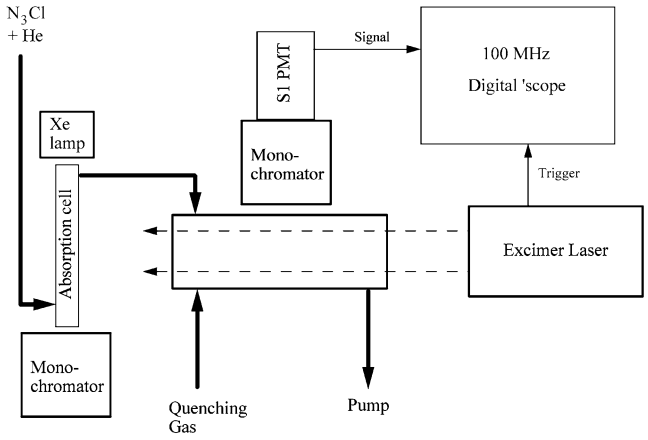

Figure 1. Apparatus used to observe the fluorescence decay and quenching of NCl(a). The absorption cell shown on the left-hand side of this diagram was used to measure the concentration of ClN_3 in the flow via the absorption band at 250 nm.

Figure 1 is a schematic diagram of the apparatus used to examine the fluorescence decay kinetics of NCl(a). A continuous flow of the He/ClN_3/Cl_2 mixture was pumped through the 5 cm diameter glass cell. The cell was equipped with quartz windows for the photolysis beam, broadband antireflection coated windows for multipass absorption measurements and a capacitance manometer for pressure measurements (MKS 390HA-00100). Typically the flow from the ClN_3 generator was around 600 sccm (including buffer gas), and the pump was throttled to give a total cell pressure in the range of 5−7 Torr.

ClN_3 was photolyzed by 10 ns pulses from an excimer laser (Lumonics TE−860−4). The laser was operated at 248 nm at a repetition rate of 5 Hz (unless otherwise stated). Photolysis laser powers were measured using a Scientec power meter at the laser output coupler. For the quenching rate constant measurements the unfocused output from the photolysis laser was used. At the center of the cell the photolysis beam had a rectangular cross section with dimensions of approximately 1 × 4 cm. To generate higher concentrations of NCl(a) for the self-annihilation rate constant measurements, the laser beam was focused by 1m focal length quartz lens. Burn patterns recorded at the focus indicated that the beam cross section had been reduced to 1 × 4 mm.

Emissions resulting from ClN_3 photolysis were dispersed by a 0.2 m monochromator. For detection of fluorescence with $\lambda > 700$ nm, a 695 nm long-pass filter was placed between the photolysis cell and the monochromator to block scattered laser light and short wavelength emission signals. This filter effectively blocked the NCl $b-X$ emission, centered at 665 nm while transmitting the $a-X$ emission at 1.08 μm. The dispersed light exiting the monochromator was detected by a cooled photomultiplier tube (Hamamatsu R1767, S1 photocathode). To record emission spectra, the output from the phototube was processed by a boxcar integrator (SRS 250). The time dependence of the fluorescence signals was examined using a digital storage oscilloscope (LeCroy ScopeStation 140, 100 MHz bandwidth). Extensive signal averaging was used to improve the signal-to-noise ratios.

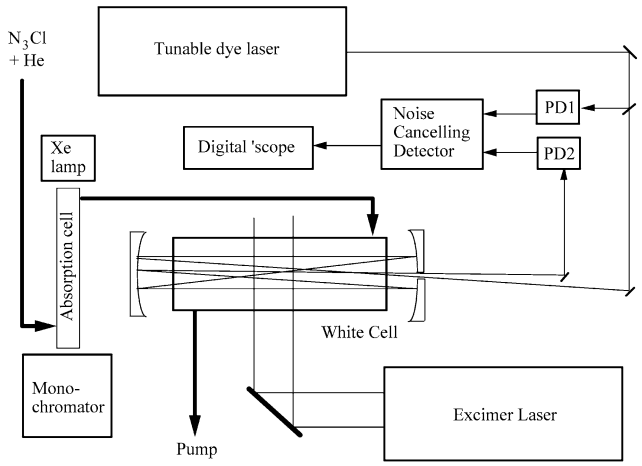

Figure 2. Apparatus used to observed the NCl $b-X$ absorption bands. The detection equipment is shown in the configuration used to observe the time dependence of the absorption signal. To record spectra the output from the NCD was processed by a boxcar integrator.

Figure 2 shows how the photolysis cell was configured for observation of the NCl $b-X$ absorption lines. The photolysis laser was not focused for the absorption measurements. For the NCl(a)/NCl branching ratio measurements oxygen was added to the photolysis cell to convert nascent NCl(a) to NCl(X) via the reaction

$$NCl(a) + O_2(X) \rightarrow NCl(X) + O_2(a) \qquad (3)$$

The O_2 flow rate was controlled by a needle valve and the partial pressure was calculated from the increase in the total cell pressure. A CW ring dye laser (Coherent 699-29) operating in the 664−666 nm range was used to record transient absorption spectra. To obtain adequate sensitivity it was necessary to compensate for intensity fluctuations in the laser output power using ratiometric detection. The probe light was split into reference and sample beams. White cell mirrors were used to obtain about 100 passes of the sample beam through the absorption cell. The sample and reference beams were then processed by a noise canceling detector (NCD) system (New Focus Nirvana detector, 125 kHz bandwidth). To record spectra, further signal-to-noise improvements were achieved by using a boxcar integrator to process the output from the NCD. Absolute calibration of the dye laser wavelength was provided by an internal wavemeter and checked against the $B-X$ lines of I_2.

Time-resolved absorption data were recorded by signal averaging the output from the NCD using the digital oscilloscope. With ClN_3 in the photolysis cell, transient changes in the intensity of the transmitted probe beam were noted when the probe laser was *not* tuned to an NCl absorption line (off-resonance signal). We attributed this signal to transient changes in the refractive index of the sample caused by local heating and the accompanying acoustic wave. The shape and magnitude of the signal changed when the laser was tuned to coincide with an NCl line. Hence, the transients associated with absorption by NCl were obtained by a subtraction technique. A signal was acquired for a preset number of photolysis pulses with the probe laser tuned on-resonance. The probe laser was then tuned off-resonance, and the signal acquired for the same number of photolysis pulses. The difference between these averaged signals defined the NCl(X) temporal profile.

Results

a. Wavelength- and Time-resolved Fluorescence. Photolysis of ClN_3 at both 193 and 248 nm produced a strong red emission in the sample cell. Dispersed fluorescence spectra confirmed that this emission originated from the $b-X$ bands of NCl. Based on the results of previous studies, it was expected that photolysis would also generate strong emissions from the NCl $a-X$ bands near 1.08 μm. Figure 3 shows spectra taken in the vicinity of the $a-X$ 0−0 band. Both photolysis wavelengths produced an intense band at 1.04 μm, which corresponds to the origin band of the N_2 $B-A$ system. The NCl $a-X$ origin band was observed at 1.077 μm. As can be seen in Figure 3, the NCl $a-X$ emission was more intense, relative to the N_2 band, for 248 nm photolysis.

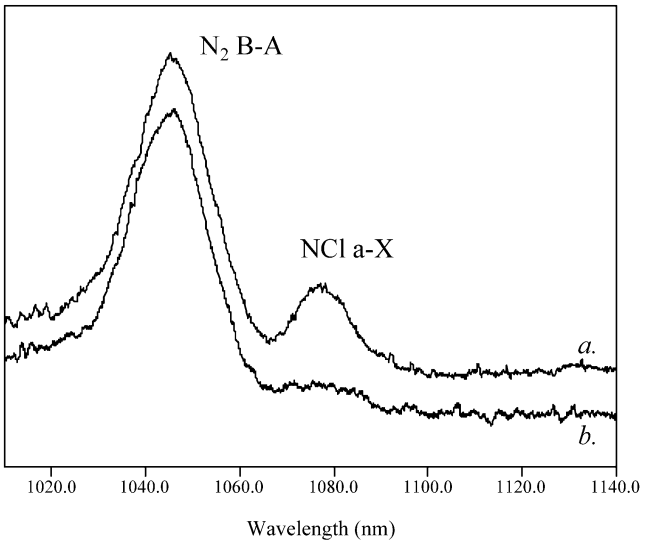

Figure 3. Emission spectra resulting from UV photolysis of ClN_3. a. Photolysis at 248 nm. b. Photolysis at 193 nm.

Fluorescence decay curves were recorded for the N_2 $B-A$ emission at 1.04 μm. These curves were multiexponential, with long-lived components that decayed over a period of 200−300 μs. They reflected the kinetics of $N_2(B)$ formation via secondary photochemical reactions. Slow decay of the N_2 $B-A$ signal imposed constraints on the conditions used to observe the decay of NCl(a). It was essential to use a monochromator transmission bandwidth that was narrow enough to isolate NCl $a-X$ from the N_2 $B-A$ emission. As this required the use of narrow slit-widths, the light collection efficiency was very low. Photolysis at 193 nm produced NCl(a) signals that were far weaker than the N_2 band. Consequently, NCl(a) decay curves obtained by 193 nm dissociation had poor signal-to-noise ratios. Better results were obtained with 248 nm photolysis. Using the unfocused output from the photolysis laser at 248 nm the NCl(a) fluorescence signals were well-represented by single-exponential decay. This was unexpected, since Ray and Coombe observed complex NCl(a) temporal profiles following 248 nm photolysis of ClN_3.

Photolysis of ClN_3 at 248 nm proved to be the most suitable source of NCl(a) for kinetic measurements in our apparatus. To avoid complications associated with NCl(a) self-annihilation, quenching rate constant measurements were carried out using low powers from the photolysis laser. Typically the energy at the center of the cell was around 20 mJ, corresponding to an irradiance of 5×10^5 W cm^{-2}. The absorption cross-section for ClN_3 at 248 nm is 3.5×10^{-18} cm^2 (base e),[9] so this power should dissociate about 2% of the azide. Quenching kinetics were characterized by recording fluorescence decay curves for a range of quenching gas pressures. For example, Figure 4 shows NCl(a) fluorescence decay curves recorded for a range of O_2 pressures. The quenching rate constants were obtained from a

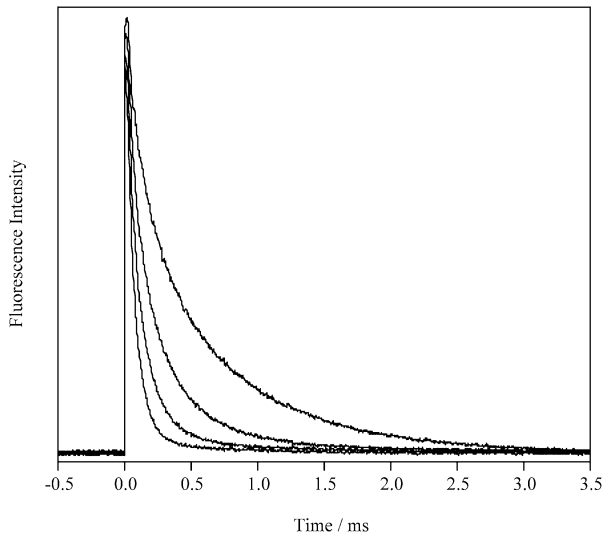

Figure 4. Fluorescence decay curves for NCl(*a*) in the presence of O_2. The intensity of the 1.077 μm $a-X$ emission was monitored. The four curves correspond to O_2 number densities of 0.0, 3.4×10^{14}, 7.4×10^{14}, and 1.5×10^{15} cm^{-3}.

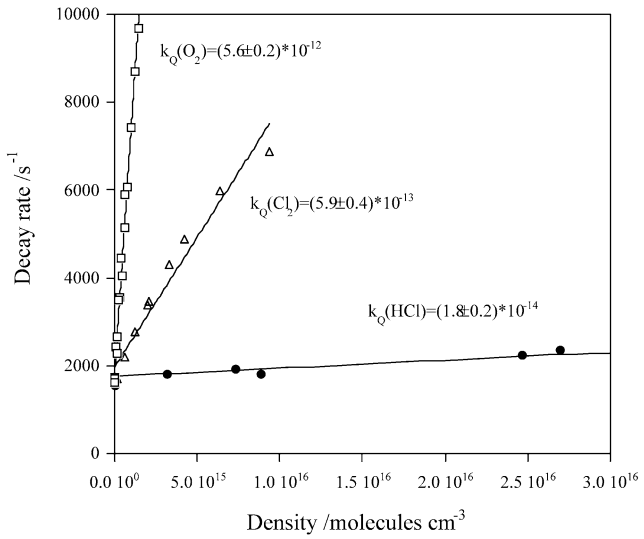

Figure 5. Stern−Volmer plots for quenching of NCl(*a*) by O_2, Cl_2, and HCl.

TABLE 1: Comparison of Rate Constants for Removal of NCl(*a*)

collision partner	rate constant /10^{-14} cm^3 s^{-1}			
	this work	ref 10	ref 5	ref 9
O_2	560 ± 40	280 ± 60	250 ± 20	
Cl_2	59 ± 8	40 ± 10	1800 ± 300	2900 ± 600
HCl	1.8 ± 0.4	1.5 ± 0.3	490 ± 70	
H_2	<0.1	<0.1	68 ± 7	
N_3Cl	30 ± 10			57 ± 4

standard Stern−Volmer analysis (decay rate vs quenching gas number density plots). A composite Stern−Volmer plot for quenching by O_2, Cl_2, and HCl is shown in Figure 5. Table 1 lists the quenching rate constants determined in this study, along with values from previous determinations.

In our experiments, quenching of NCl(*a*) by H_2 was so slow that we were unable to determine the rate constant. This observation was in agreement with the results of Hewett et al.,[10] while the measurements of Ray and Coombe[5] yielded a quenching rate constant of $(6.8 \pm 0.7) \times 10^{-13}$ cm^3 s^{-1}. To investigate this discrepancy we examined the quenching of NCl(*a*) by H_2 using 193 nm of ClN_3. Measurements made using the monochromator to isolate the NCl $a-X$ emission showed no influence of added H_2 on the long-lived component of the fluorescence. In contrast, when the monochromator was set to transmit the N_2 $B-A$ fluorescence at 1.04 μm, the long-lived component of the decay was quenched by H_2. These experiments were repeated using an interference filter to restrict the range of wavelengths reaching the detector. The filter, obtained on loan from Professor Coombe, had a transmission maximum at 1.08 μm and a bandwidth of 12 nm. Fluorescence decay curves that were observed through this filter were similar to those obtained when the monochromator was used to select the N_2 $B-A$ emission, and the addition of H_2 resulted in quenching of this fluorescence.

Studies of NCl(*a*) self-annihilation were carried out using relatively high powers from the photolysis laser, and focusing of the beam. The energies delivered to the center of the cell ranged from 5 to 45 mJ per pulse, corresponding to irradiances of $1.3 \times 10^7-1.1 \times 10^8$ W cm^{-2}. Figure 6a,b show examples of NCl(*a*) fluorescence decay curves recorded at different photolysis laser powers. All of the curves exhibited a fast spike near zero time, which was caused by scattered light from the photolysis laser. Figure 6a illustrates results for low to moderate laser powers. Here it can be seen that the intensity of the fluorescence increases as the laser power increases, as does the initial decay rate (after the laser spike). With further increases in laser power the signal grew at a rate that was less than linearly dependent on the power. Eventually both the intensity and the temporal profile of the signal became independent of laser power. This situation is illustrated by the data in Figure 6b, where almost identical curves are shown for three different laser powers. We ascribe the limiting high-power behavior to complete dissociation of the ClN_3 within the region viewed by the detection system. As noted in the Introduction, this is a desirable situation as the concentration of NCl(*a*) can be determined, provided that the initial concentration of ClN_3 and the branching fraction for NCl(*a*) production are known. It should be noted that multiphoton dissociation and ionization processes could become increasingly more important as the laser intensity is increased. However, the fact that the NCl(*a*) fluorescence decay curves did not depend on the laser power over the range from 33 to 44 mJ (cf. Figure 6b) indicates that multiphoton processes did not influence the decay kinetics to a measurable degree.

The 250 nm absorption measurement gives the concentration of ClN_3 entering the photolysis cell, but this is not necessarily the initial concentration. The flow of gas through the photolysis cell was relatively slow, requiring about 5 s for complete replenishment. Hence, measurements made at high pulse repetition rates could suffer from local depletion of ClN_3 by preceding photolysis pulses. To test for this effect we recorded fluorescence decay curves using pulse repetition rates in the range from 0.2 to 10 Hz. Within this range the curves were not dependent on the repetition frequency, indicating that diffusion was fast enough to replace the ClN_3 between laser shots.

b. Transient Absorption of NCl(*X*). Searches for the NCl $b-X$ absorption lines near 665 nm were made using photolysis of ClN_3/O_2/He mixtures in the apparatus shown in Figure 2. O_2 was added to increase the concentration of NCl(*X*). An example of the $b-X$ absorption spectrum, recorded by scanning the dye laser over the range from 15048.0 to 15051.0 cm^{-1}, is shown in Figure 7. Note that the signal-to-noise ratio of this trace was limited by the scanning electronics that control the dye laser. The minimum sweep speed was not slow enough to

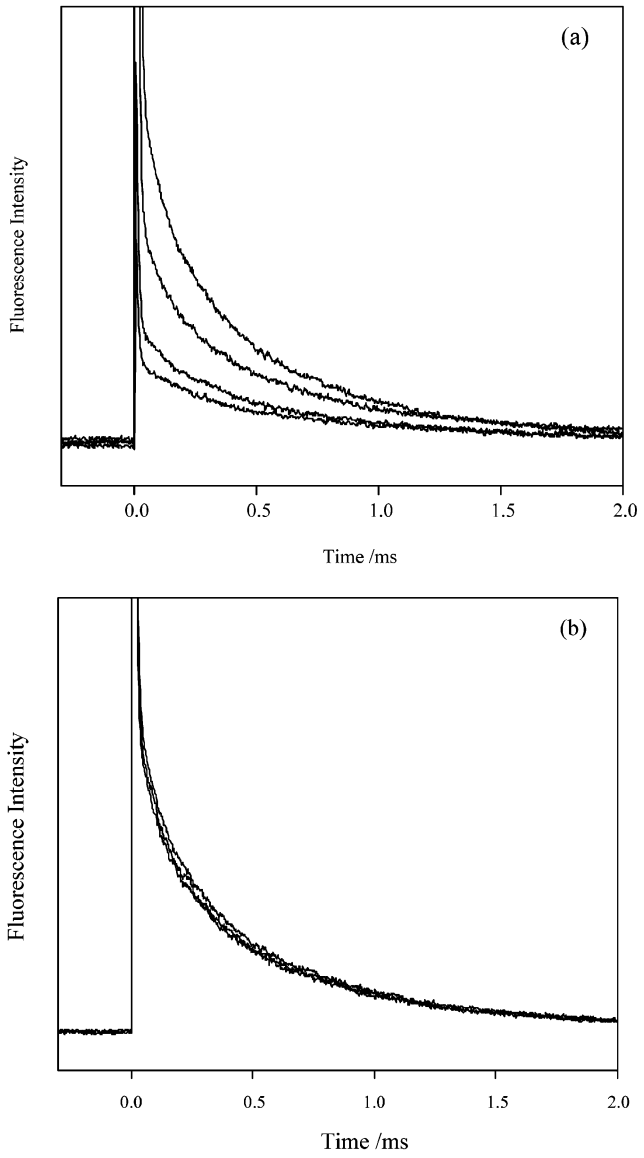

Figure 6. (a) Fluorescence decay curves for NCl(a) using moderate laser powers to dissociate ClN_3. The intensity of the 1.077 μm $a-X$ emission was monitored. These curves were recorded with the gain of the detection system held constant. The fast spike at beginning of each curve is due to scattered laser light. The laser pulse energies for these curves were 4.2, 6.6, 12, and 24 mJ. (b) NCl(a) fluorescence decay curves recorded using high photolysis laser powers. The three curves shown here were recorded using pulse energies of 33, 39, and 44 mJ at the center of the cell.

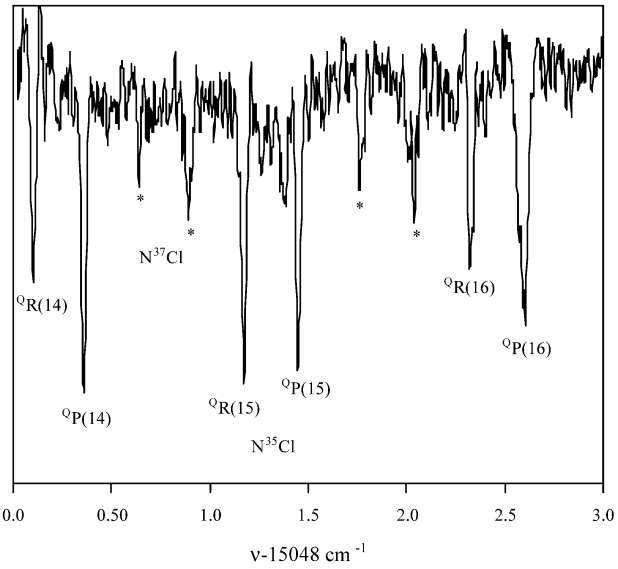

Figure 7. Segment of the NCl $b-X$ 0−0 absorption band. This was recorded by scanning the dye laser over the range from 15048.0 to 15051.0 cm^{-1}.

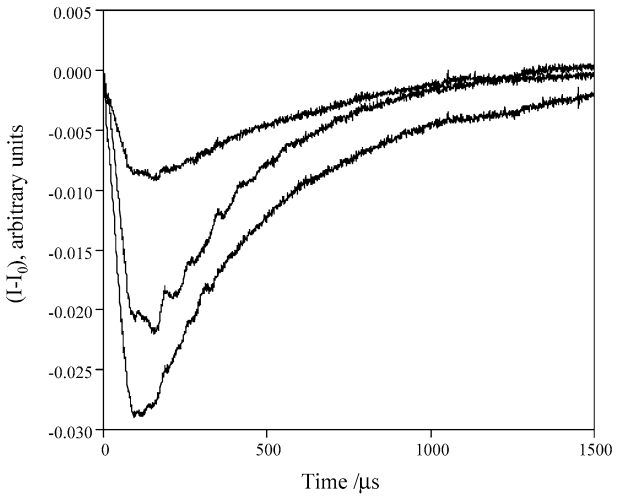

Figure 8. Transient NCl(X) absorption signals obtained by photolysis of ClN_3 in the presence of O_2. These traces were recorded by monitoring the absorption of the ^{Q}P(14) line. They correspond to O_2 densities of 0, 8.4×10^{15} and 1.9×10^{16} cm^{-3}. The amplitude of the absorption increases with increasing [O_2].

permit extensive signal averaging. The relative positions of the $b-X$ 0−0 band rotational lines were in excellent agreement with the work of Colin and Jones.[22] However, we found a small systematic calibration error in the former study. Our measurements indicate that the line positions of Colin and Jones[22] should be reduced by 0.04 cm^{-1}. Although small, this correction is of significance for the development of diode laser diagnostic instruments. Figure 7 and similar spectra were recorded in the presence of 6 Torr of buffer gas (mostly He), with a 100 μs delay between the photolysis pulse and the absorption measurement. Under these conditions the rotational and translational energy of NCl should be in thermal equilibrium with the buffer gas. This was confirmed by the rotational line intensity distribution, which defined a rotational temperature of 300 ± 20 K. The translational temperature was estimated from absorption line profiles. The line shapes were well represented by a Gaussian function with a line width of 0.031 cm^{-1} (fwhm). This is slightly wider than would be expected for a temperature of 300 K (predicted width of 0.026 cm^{-1}).

Searches were made for transitions originating from vibrationally excited levels of NCl(X), to examine the possibility that vibrationally excited products are produced (and survive multiple collisions with He) after photolysis of ClN_3. We were unable to detect population in the $v = 1$ or 2 levels using 248 nm photolysis. From these measurements, and estimates of the sensitivity of the apparatus, we conclude that >80% of the nascent NCl(X) had undergone vibrational relaxation, if a nonequilibrium vibrational distribution had been created in the first instance.

Figure 8 shows examples of time-resolved absorption traces. These curves were recorded for a range of added O_2 pressures. Here it can be seen that the maximum concentration of NCl(X) increased as O_2 was added to the mixture. This effect suggests that collisions with O_2 quenched NCl(a) to NCl(X), thereby reducing the amount of NCl(a) lost to reactive channels. In

keeping with this interpretation it was found that the influence of added O_2 saturated for partial pressures above 0.2 Torr.

Analysis

a. NCl(X) Kinetics and the Branching Fraction for Formation of NCl(a). As described in the Introduction, the primary products resulting from photolysis of ClN_3 at 248 nm are NCl(a)+N_2 and NCl(X)+N_2. To establish the initial concentration of NCl(a) formed, the branching fraction $f = [NCl(a)]_0/([NCl(a)]_0 + [NCl(X)]_0)$ was derived from the transient absorption data. The reactions that are of importance in determining the NCl(X) time profiles are

$$NCl(a) + ClN_3 \rightarrow NCl(X) + ClN_3 \quad (4a)$$

$$NCl_2 + N_3 \quad (4b)$$

$$NCl(a) + Cl_2 \rightarrow NCl_2 + Cl \quad (5)$$

$$NCl(X) + NCl(X) \rightarrow N_2 + 2Cl \quad (6)$$

$$NCl(X) + ClN_3 \rightarrow \text{products} \quad (7)$$

and reaction 3. The rate constants k_3, ($k_{4a} + k_{4b}$), and k_5 are given in Table 1. The NCl(X)+NCl(X) removal rate constant ($k_6 = 8 \times 10^{-12}$ cm^3 s^{-1}) was measured by Clyne and MacRobert.[2] For completeness, reaction 1, the self-annihilation of NCl(a), was included in the analysis. However, this reaction did not contribute significantly under the conditions of the absorption measurements (NCl(a) fluorescence decay curves were single exponential for these conditions). An initial estimate of the branching fraction can be derived from a simplified analysis of the absorption curves shown in Figure 8. The absence of NCl(X) absorption immediately after the photolysis pulse gives the appearance that there is no prompt production of NCl(X) (i.e., $f \approx 1$). However, this observation could be misleading as it ignores ro-vibrational relaxation within the ground-state manifold (which matters as we were monitoring a single ro-vibrational state) and the finite response time of the detection system (8 μs rise time). First consider the curve for the system with no added O_2. The growth in the NCl(X) signal could be attributed to ro-vibrational relaxation of the initially "hot" NCl(X) and population transferred down from NCl(a) by reaction 4a. For the moment we assume that all of the NCl(a) is being removed by some other process, and there is no downward transfer. In this rather extreme view the NCl(X) signal rises in response to ro-vibrational relaxation and decays as NCl(X) is lost through reactions 6, 7, and diffusion. The maximum in this curve is then proportional to the initial concentration of NCl(X) formed. Next, we make the assumption that a moderate pressure of O_2 can overwhelm reactive loss of NCl(a), and transfer all of the excited-state population to the ground state via reaction 3. This approximation can be validated by considering the kinetics for the typical measurement conditions. The relevant concentrations are $[ClN_3] = 10^{16}$, $[Cl_2] = 5 \times 10^{14}$, and $[O_2] = 6 \times 10^{15}$ cm^{-3}. Reactions 4a,b and 5 remove NCl(a) at a rate of 3300 s^{-1}, while O_2 transfers population to the ground state at a rate of 34000 s^{-1}. For such limiting conditions, the maximum absorbance of the curve recorded in the presence of O_2 is proportional to the concentration of NCl formed by photolysis ($[NCl(a)]_0 + [NCl(X)]_0$). With this interpretation the data for $[O_2] = 0$ and $[O_2] = 1.9 \times 10^{16}$ cm^{-3} yield a branching fraction of $f = 0.7$. Because collisions between NCl(a) and ClN_3 or Cl_2 may also cause some downward transfer, thereby influencing the $[O_2] = 0$ data, the value of 0.7 should be regarded as a lower limit. Clearly, a better estimate for f should be obtained by using numerical integration of the rate equations for the scheme represented by reactions 1 and 3−7 to simulate the absorption curves. This was done using f and k_7 (which had not been determined previously) as variable parameters. The best fit was obtained for $f \geq 0.9$ and $k_7 = 2.5 \times 10^{-13}$ cm^3 s^{-1}.

In the analysis presented so far we have not considered chain decomposition of ClN_3. Ray and Coombe[5] observed NCl(a) fluorescence signals that appeared to reflect chain decomposition of ClN_3 when 248 nm light was used for photolysis. They suggested that the chain is carried by the reaction

$$NCl(a) + ClN_3 \rightarrow NCl(a) + NCl(X) + N_2(v) \quad (8)$$

In a recent study of ClN_3 decomposition, Jensen et al.[18] proposed that reaction 8 proceeds with a rate constant of 2.0×10^{-12} cm^3 s^{-1}. Clearly, the above analysis of the branching fraction would be in error if chain reactions were of importance. We explored this possibility by including reaction 8 in our kinetic model. With this addition the behavior of the model was very different from the experimental observations. Addition of O_2 to the system was predicted to reduce the amount of NCl(X) observed, as it suppressed production from the chain reaction. A possible solution to this problem is to assume that the $O_2(a)$ generated by reaction 3 can also dissociate ClN_3, e.g.,

$$O_2(a) + ClN_3 \rightarrow O_2(X) + NCl(a) + N_2 \quad (9)$$

Ray and Coombe[5] proposed a rate constant of 1.7×10^{-11} cm^3 s^{-1} for this process. When this reaction was included in the model it had a large impact on the rate at which O_2 appeared to quench NCl(a). For the range of conditions used to record the fluorescence decay curves shown in Figure 4, the model predicted an effective fluorescence decay rate for NCl(a) that was almost independent of the O_2 concentration.

We made several attempts in our experiments to observe photoinitiated chain decomposition of ClN_3, for gas mixtures with and without O_2. No evidence for chain decomposition could be found, and kinetic models that included chain propagation steps were not consistent with the observed time histories for NCl(a) and NCl(X). We concluded that reactions 3−7 provide an adequate description of the kinetics for our measurement conditions, and that a lower bound for the NCl(a) branching fraction of $f > 0.7$ is conservative.

b. Self-Annihilation of NCl(a). The decay curves used to examine NCl(a) self-annihilation were recorded under conditions where only He, ClN_3, and Cl_2 were present in the cell prior to the photolysis pulse. Hence, the removal of NCl(a) was governed by reactions 1, 4a, 4b, 5, and diffusion (the loss by diffusion was noticeable in the self-annihilation measurements as the fluorescence from a small photolysis volume was imaged). Henshaw et al.[9] considered the same set of reactions in their study of self-annihilation. Integration of the rate equation for NCl(a) gives the expression

$$[NCl(a)] = \frac{k_L[NCl(a)]_0}{\exp(k_L t)(k_1[NCl(a)]_0 + k_L) - k_1[NCl(a)]_0} \quad (10)$$

where k_L is the sum of the first-order loss processes,

$$k_L = (k_{3a} + k_{3b})[ClN_3] + k_4[Cl_2] + \Gamma_d \quad (11)$$

and Γ_d is the diffusion loss rate. The decay curves recorded using high photolysis laser powers were very well-represented

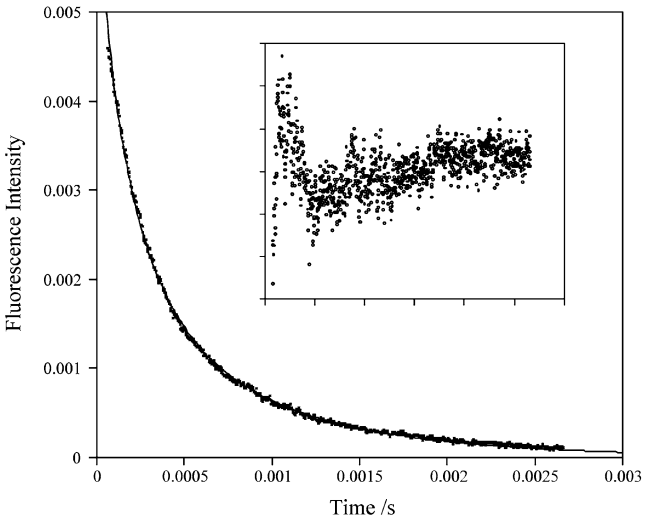

Figure 9. Example showing the fit of eq 10 to an NCl(a) fluorescence decay curve recorded using high irradiance photolysis of ClN_3. The inset shows the residuals for the fitted function.

by eq 10. An example of the quality of the fit is shown in Figure 9. Because k_1 cannot be obtained independently from this type of measurement, it was determined by fitting with $[NCl(a)]_0$ held constant. To have the best definition of this parameter we began by analyzing the data for which >95% of the ClN_3 had been photodissociated. We then assumed that 90% of the products resulted from fragmentation to NCl + N_2, and that 80% of the NCl was NCl(a). This gives $[NCl(a)]_0 = 0.7[ClN_3]_{t<0}$, where $[ClN_3]_{t<0}$, is the concentration of ClN_3 prior to photolysis. Fitting seven different curves recorded with laser pulse energies in excess of 30 mJ per pulse yielded a self-annihilation rate constant of $(6.7 \pm 0.7) \times 10^{-13}$ cm^3 s^{-1}. This analysis was extended to include data taken under conditions where ClN_3 was not completely dissociated. For these data we used the laser power measurements and the absorption cross-section for ClN_3 at 248 nm to determine $[NCl(a)]_0$. Analysis of all of the curves recorded with moderate to high laser irradiances yielded a self-annihilation rate constant of $(7.0 \pm 1.5) \times 10^{-13}$ cm^3 s^{-1}. The error range includes a conservative estimate for uncertainty in the NCl(a) branching fraction.

Discussion

The NCl(a) quenching rate constants from the present work are compared with values from previous studies in Table 1. Here it can be seen that our results are much closer to the rate constants obtained from flow tube experiments[10] than those from studies that used ClN_3 photolysis to generate NCl(a).[9,5] The biggest discrepancy between the present study and the flow tube results is for O_2. This is curious, as the O_2 quenching rate constant was the only point of agreement between the flow tube and earlier photolysis experiments. Our measurement was repeated several times, and the values obtained were always outside the error ranges of the previous determinations. However, the factor of 2 discrepancy for O_2 is not as troubling as the orders of magnitude differences between flow tube and photolysis results that had been encountered for other quenchers (cf. Table 1).

It was surprising to find large differences between the present 248 nm photolysis results and previous measurements made using 193 nm photolysis. Chain dissociation of ClN_3 did not appear to be a problem in our system. For low photolysis laser irradiances the NCl(a) fluorescence decay curves were exponential, and the decay rates yielded linear Stern−Volmer plots. In the work of Ray and Coombe[5] and Henshaw et al.,[9] an interference filter was used to isolate the NCl($a-X$) emission. We had speculated that this filter may have transmitted radiation from other emitting species as well as NCl(a). Jansen et al.[18] argued that the 12 nm band pass of their filter would be sufficient to eliminate interference form N_2 emission, but experiments with this filter in our apparatus yielded results that were significantly influenced by incomplete suppression of the N_2 $B-A$ emission.

Given that most of our first-order rate constants for removal of NCl(a) differ from those of Henshaw et al.[9] it is not surprising to find that the self-annihilation rate constants are also in conflict. Our value is an order of magnitude smaller. Even the data taken at low laser irradiances were at variance with the larger value for k_1. Consider the decay curve in Figure 4 that was recorded with no O_2 present in the system. This curve is consistent with a single-exponential function that decays with a rate of 1900 s^{-1}. For the conditions of this measurement the initial concentration of NCl(a) was 2×10^{14} cm^{-3}. If we assume Henshaw et al.'s[9] value for k_1, the initial rate of decay due to the second-order removal process alone would be 1400 s^{-1}. This is three-fourths of the total decay rate and would result in a distinctly nonexponential decay curve, contrary to the observed behavior. The present value for k_1 yields an initial second-order decay rate 140 s^{-1}, which is compatible with the data shown in Figure 4.

As k_1 and $[NCl(a)]_0$ are inversely proportional, the k_1 value would have been underestimated if the branching fraction for NCl(a) formation were overestimated. If we assume Henshaw et al's[9] value for k_1 the corresponding branching fraction for NCl(a) production would be just 0.07. Such a low value is incompatible with previous studies of ClN_3 photolysis that are consistent in finding that NCl(a) + N_2 is the dominant product channel.

The fact that we were unable to observe secondary NCl(a) generated by chain decomposition of ClN_3 is puzzling. Jensen et al.[18] examined this process by recording the time history of ClN_3 following 248 nm photolysis. They observed removal of ClN_3 by secondary reactions that lasted for about 500 μs. Approximately 3% of the azide was initially dissociated, and it appeared that about 12% of the azide was consumed by the time the secondary reactions terminated. Loss of ClN_3 was attributed to reactions 4b, 7 and dissociation of ClN_3 caused by successive collisions with N_2(v). Jensen et al.[18] modeled the ClN_3 removal kinetics, and proposed rate constant values of $k_{4b} = 1.5 \times 10^{-12}$ and $k_8 = 2.0 \times 10^{-12}$ cm^3 s^{-1}. Their model included self-annihilation of NCl(a) with the rate constant from the work of Henshaw et al.[9] The proposed values for k_{4b} and k_8 are not supported by the present study. Quenching of NCl(a) by ClN_3 occurred with a rate constant of $k_{4b} = (3 \pm 1) \times 10^{-13}$ cm^3 s^{-1}. The problems posed by reaction 8 were discussed above as part of the analysis of the NCl(X) transient absorption data. While the data presented by Jensen et al.[18] clearly show reactive removal of ClN_3, the mechanism proposed for this process cannot reproduce the observed kinetics when the rate constants determined in the present study are used. Our data indicate that a different mechanism is operative, which does not generate detectable quantities of NCl(a).

Summary and Conclusions

Photolysis of ClN_3 and the kinetics of NCl(a, X) were investigated using time-resolved emission and absorption tech-

niques. Pulsed photolysis of ClN_3 at 248 nm was used to generate NCl(a) for kinetic measurements. Rate constants for quenching by O_2, H_2, Cl_2, HCl, and ClN_3 were determined. The values obtained were in agreement with results from flow tube measurements,[10] but differed greatly from rate constants determined previously using photolysis of ClN_3 at 193 nm as the source of NCl(a).[9,5]

Time-resolved NCl(X) concentration profiles were recorded following 248 nm photolysis of ClN_3. Information regarding the decay of NCl(a) was implicit in these data when collisional transfer to the ground state occurred. This circumstance was used to evaluate the branching fraction for NCl(a) production. Collisions with O_2 were used to quench the NCl(a). Kinetic modeling of the associated NCl(X) absorption profiles yielded a lower bound for the $ClN_3 + 248\ nm \rightarrow NCl(a) + N_2$ branching fraction of 70%.

Removal of NCl(a) by self-annihilation was examined using intense photolysis pulses to generate high concentrations of NCl(a). The initial concentration was determined by achieving complete dissociation of ClN_3. Decay curves that exhibited obvious second-order decay characteristics were recorded. Analysis of these data yielded a self-annihilation rate constant of $(7.0 \pm 1.5) \times 10^{-13}$ cm^3 s^{-1}. This value is an order of magnitude smaller than previous estimates,[3,9] and it indicates that transport losses of NCl(a) in chemical laser systems will not be as severe as had been thought previously.

Acknowledgment. We are grateful to Professor Robert D. Coombe (Denver University) for helpful discussion concerning the photodissociation dynamics of ClN_3 and for loan of the interference filter used in some of the measurements. We also thank AFRL/ Kirtland AFB for supplying the S1 photomultiplier used in these measurements. This work was supported by the Air Force Office of Scientific Research under grant F49620-01-1-0070.

References and Notes

(1) Clyne, M. A. A.; MacRobert, A. J.; Brunning, J.; Cheah, C. T. *J. Chem. Soc., Faraday Trans. 2* **1983**, *79*, 1515−24.
(2) Clyne, M. A. A.; MacRobert, A. J. *J. Chem. Soc., Faraday Trans. 2* **1983**, *79*, 283−93.
(3) Benard, D. J.; Chowdhury, M. A.; Winker, B. K.; Seder, T. A.; Michels, H. H. *J. Phys. Chem.* **1990**, *94*, 7507−14.
(4) Ray, A. J.; Coombe, R. D. *J. Phys. Chem.* **1993**, *97*, 3475−9.
(5) Ray, A. J.; Coombe, R. D. *J. Phys. Chem.* **1994**, *98*, 8940−5.
(6) Ray, A. J.; Coombe, R. D. *J. Phys. Chem.* **1995**, *99*, 7849−52.
(7) Schwenz, R. W.; Gilbert, J. V.; Coombe, R. D. *Chem. Phys. Lett.* **1993**, *207*, 526−30.
(8) Henshaw, T. L.; Herrera, S. D.; Schlie, L. A. *J. Phys. Chem. A* **1998**, *102*, 6239−46.
(9) Henshaw, T. L.; Herrera, S. D.; Haggquist, G. W.; Schlie, V. A. *J. Phys. Chem. A* **1997**, *101*, 4048−56.
(10) Hewett, K. B.; Manke, G. C., II.; Setser, D. W.; Brewood, G. *J. Phys. Chem. A* **2000**, *104*, 539−551.
(11) Manke, G. C., II.; Setser, D. W. *J. Phys. Chem. A* **1998**, *102*, 7257−7266.
(12) Yang, T. T.; Gylys, V. T.; Bower, R. D.; Rubin, L. F. *Opt. Lett.* **1992**, *17*, 1803−5.
(13) Bower, R. D.; Yang, T. T. *J. Opt. Soc. Am. B: Opt. Phys.* **1991**, *8*, 1583−7.
(14) Herbelin, J. M.; Henshaw, T. L.; Rafferty, B. D.; Anderson, B. T.; Tate, R. F.; Madden, T. J.; Manke, G. C., II; Hager, G. D. *Chem. Phys. Lett.* **1999**, *299*, 583−588.
(15) Henshaw, T. L.; Manke, G. C., II; Madden, T. J.; Berman, M. R.; Hager, G. D. *Chem. Phys. Lett.* **2000**, *325*, 537−544.
(16) Manke, G. C.; Henshaw, T. L.; Madden, T. J.; Hager, G. D. *Chem. Phys. Lett.* **1999**, *310*, 111−120.
(17) Komissarov, A. V.; Manke, G. C., II; Davis, S. J.; Heaven, M. C. *Proc. SPIE−Int. Soc. Opt. Eng.* **2000**, *3931*, 138−148.
(18) Jensen, R. H.; Mann, A.; Coombe, R. D. *J. Phys. Chem. A* **2000**, *104*, 6573−6579.
(19) Coombe, R. D.; Patel, D.; Pritt, A. T., Jr.; Wodarczyk, F. J. *J. Chem. Phys.* **1981**, *75*, 2177−90.
(20) Lock, M.; Gericke, K.-H.; Comes, F. J. *Chem. Phys.* **1996**, *213*, 385−396.
(21) Heaven, M. C. Experimental and theoretical Studies of NCl Kinetics. Annual Report for AFOSR; Grant F49620-01-1-0070, August, 2001.
(22) Colin, R.; Jones, W. E. *Can. J. Phys.* **1967**, *45*, 301.